



ELSEVIER

Available online at www.sciencedirect.com

SCIENCE @ DIRECT®

Journal of Sound and Vibration 280 (2005) 415–424

JOURNAL OF
SOUND AND
VIBRATION

www.elsevier.com/locate/jsvi

Short Communication

Design of bidirectional functionally graded plate for optimal natural frequencies

L.F. Qian^a, R.C. Batra^{b,*}

^a*Nanjing University of Science and Technology, Nanjing 210094, PR China*

^b*Department of Engineering Science and Mechanics, Virginia Polytechnic Institute and State University, Blacksburg, VA 24061, USA*

Received 14 January 2004; accepted 28 January 2004

Available online 8 October 2004

1. Introduction

An advantage of functionally graded materials (FGMs) over laminated composites is that material properties vary continuously in an FGM but are discontinuous across adjoining layers in laminated composites. Furthermore, in an FGM material, properties can be graded in all three directions which is more difficult to achieve in laminated composites. FGMs have been used for structural optimization, e.g., bamboo is a highly optimized naturally occurring FGM [1]. FGMs with material properties varying only in the thickness direction can be manufactured by high-speed centrifugal casting [2,3], or by depositing ceramic layers on a substrate [4,5], and those with properties varying in the plane of a sheet by ultraviolet irradiation to alter the chemical composition [6].

Plate theories used to analyze deformations of an FG plate include the first-order shear deformation theory (FSDT) [7], the third-order shear deformation theory (TSDT) [8], and the compatible higher-order shear and normal deformation plate theory (HOSNDPT) [9–11]. In the FSDT and the TSDT three-dimensional constitutive relations are modified by assuming that the transverse normal stress vanishes. After solving the plate theory equations, the transverse shear and the transverse normal stresses are computed first by finding the in-plane stresses and then

*Corresponding author. Tel.: +1-540-2316051; fax: +1-540-2314574.

E-mail address: rbatra@vt.edu (R.C. Batra).

integrating through the thickness the balance of linear momentum. The HOSNDPT accounts for both transverse shear and transverse normal stresses and these are computed from equations of the plate theory [12,13].

Whereas the finite element method (FEM) has often been used to find an approximate solution of an initial-boundary-value problem and for finding frequencies, the use of meshless methods for finding approximate solutions of these problems has been gaining popularity. Two recent books [14,15] summarize developments in meshless methods.

Here we use the meshless local Petrov–Galerkin (MLPG) [14,15] method and the compatible HOSNDPT to design a thick two-constituent FG cantilever plate having either the highest first natural frequency or the highest second natural frequency; a comparison of the MLPG and the FE methods is given in Ref. [16,17]. The volume fraction of a constituent is assumed to vary in x - and y -directions. The two constituents and the macroscopic response of the beam are assumed to be isotropic with effective elastic moduli deduced by the Mori–Tanaka [18] technique. The spatial volume fractions of the two constituents are optimized so as to maximize either the first or the second natural frequency of the structure.

The transient response of an optimized plate to uniformly distributed time-dependent loads applied on its top surface is compared with that of two homogeneous plates comprised of each material.

2. Formulation of the problem

2.1. Governing equations

A schematic sketch of the problem studied and the rectangular Cartesian coordinates used to describe its deformations are given in Fig. 1. Neglecting body forces, transient deformations of a plate are governed by

$$\begin{aligned}
 \sigma_{ij,j} &= \rho \ddot{u}_i \text{ in } \Omega \times (0, T), & \sigma_{ij}n_j &= \bar{f}_i \text{ on } \Gamma_f \times [-h/2, h/2] \times (0, T), \\
 u_i &= \bar{u}_i \text{ on } \Gamma_u \times [-h/2, h/2] \times (0, T), & \sigma_{ij}n_j &= q_i^\pm \text{ on } S^\pm \times (0, T), \\
 u_i(x, y, z, 0) &= u_i^0(x, y, z) \text{ in } \Omega, & \dot{u}_i(x, y, z, 0) &= \dot{u}_i^0(x, y, z) \text{ in } \Omega.
 \end{aligned}
 \tag{1}$$

Here ρ is the mass density, div the three-dimensional divergence operator, $\Omega = [0, \ell] \times [0, b] \times [-h/2, h/2]$ the region occupied by the plate in the reference configuration, and \mathbf{n} an outward unit

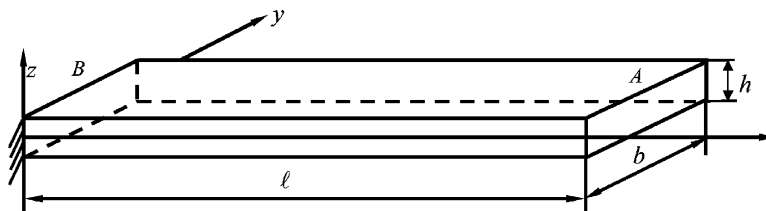


Fig. 1. Schematic sketch of the problem studied.

normal to the boundary $\partial\Omega$ of Ω . S^+ and S^- are the top and the bottom surfaces of the plate where surface tractions are prescribed, respectively, as \mathbf{q}^+ and \mathbf{q}^- . Γ_u and Γ_f are parts of the boundary ∂S of the midsurface S . On $\Gamma_u \times [-h/2, h/2]$ and $\Gamma_f \times [-h/2, h/2]$ displacements and surface tractions are prescribed as $\bar{\mathbf{u}}$ and $\bar{\mathbf{f}}$, respectively. A repeated index implies summation over the range of the index, and $\sigma_{ij,k} = \partial\sigma_{ij}/\partial x_k$. Eq. (1)₁ is the balance of linear momentum, Eqs. (1)₂–(1)₄ are boundary conditions, and Eqs. (1)₅ and (1)₆ are initial conditions. When studying free vibrations of a cantilever plate, we set

$$\bar{\mathbf{f}} = \mathbf{q}^\pm = \mathbf{0}, \quad \bar{\mathbf{u}} = \mathbf{0} \quad \text{on the fixed edge,} \tag{2}$$

$$\mathbf{u}(x, y, z, t) = e^{i\omega t} U(x, y, z), \tag{3}$$

and neglect initial conditions (1)₅ and (1)₆. In Eq. (3), ω is a natural frequency. Stresses $\boldsymbol{\sigma}$ at a point are related to infinitesimal strains $\boldsymbol{\varepsilon}$ there by

$$\sigma_{ij} = (K_e - \frac{2}{3}\mu_e)\varepsilon_{kk}\delta_{ij} + 2\mu_e\varepsilon_{ij}, \tag{4}$$

where K_e and μ_e are, respectively, the effective bulk and the effective shear moduli of the two-constituent plate, and δ_{ij} is the Kronecker delta. They are related to the elastic moduli (K_1, μ_1) and (K_2, μ_2) of the constituents by [18]

$$\frac{K_e - K_1}{K_2 - K_1} = \frac{V_2}{1 + (1 - V_2)[3(K_2 - K_1)/(3K_1 + 4\mu_1)]},$$

$$\frac{\mu_e - \mu_1}{\mu_2 - \mu_1} = \frac{V_2}{1 + (1 - V_2)(\mu_2 - \mu_1)/[\mu_1 + \mu_1(9K_1 + 8\mu_1)/6(K_1 + 2\mu_1)]}, \tag{5}$$

where V_2 is the volume fraction of constituent 2. We assume that

$$V_2(x, y, z) = \left(\frac{1}{2} + \frac{z}{h}\right)^p \left(\frac{x}{\ell}\right)^q, \tag{6}$$

where parameters p and q control the volume fraction profile of the constituent 2 in the xz -plane.

2.2. Displacement field in the HOSNDPT

Let $L_1(z), L_2(z), \dots$ be orthonormalized Legendre polynomials defined on $[-h/2, h/2]$. That is

$$\int_{-h/2}^{h/2} L_i(z)L_j(z) dz = \delta_{ij}. \tag{7}$$

Note that $L_i(z)$ has dimensions of $(\text{length})^{-1/2}$. We expand the displacement field \mathbf{u} as

$$\mathbf{u}(x, y, z, t) = \sum_{i=0}^K L_i(z)\mathbf{d}^{(i)}(x, y, t), \tag{8}$$

where $\mathbf{d}^{(i)}$ denote time-dependent displacements of a point on the midsurface of the plate and have dimensions of $(\text{length})^{3/2}$. Previous work [9–11] with thick plates has revealed that $K = 5$ gives results in close agreement with the analytical solution. We refer the reader to Refs. [12,13] for a

derivation of equations of the mixed and the compatible HOSNDPT; we adopt the latter theory here. When studying free vibrations of a plate, we set

$$\mathbf{d}^{(i)}(x, y, t) = e^{i\omega t} \mathbf{D}^{(i)}(x, y). \tag{9}$$

2.3. Semidiscrete formulation

Let M nodes be placed on the midsurface S of the plate, and S_1, S_2, \dots, S_M be smooth two-dimensional closed regions, not necessarily disjoint and of the same shape and size, enclosing nodes $1, 2, \dots, M$, respectively. Let ϕ_1, ϕ_2, \dots be linearly independent functions defined on one of these regions, say S_α ; these are derived by the moving least-squares approximation [19] and using fourth-order polynomials as weight functions. For a K th order plate theory there are $3(K + 1)$ unknowns $d_1^{(0)}, d_2^{(0)}, d_3^{(0)}, d_1^{(1)}, d_2^{(1)}, d_3^{(1)}, \dots, d_1^{(K)}, d_2^{(K)}, d_3^{(K)}$ at every point in S and hence in S_α . We write these as a $3(K + 1)$ dimensional array $\{d\}$, and set

$$\{d(x, y, t)\} = \sum_{J=1}^N [\phi_J(x, y)]\{\delta_J(t)\}, \tag{10}$$

where, for each value of J , $\{\delta_J\}$ is a $3(K + 1)$ -dimensional array and $[\phi_J]$ is a square matrix of $3(K + 1)$ rows. Note that $\{\delta_J\}$ are functions of time t .

In the MLPG method one derives a weak formulation of the governing equations (1)₁ on S_α without requiring the test function to satisfy any conditions on ∂S_α . Essential boundary conditions (1)₃ are satisfied either by using the penalty method, or by the method of Lagrange multipliers, or by appropriately modifying the mass and the stiffness matrices.

There is no assembly of equations required in the MLPG method. The end result is a system of coupled ordinary differential equations (e.g. see Refs. [9–11])

$$\mathbf{M}\ddot{\delta} + \mathbf{K}\delta = \mathbf{F}, \tag{11}$$

where \mathbf{M} is the mass matrix, \mathbf{K} the stiffness matrix, and \mathbf{F} the load vector.

Eqs. (11) are integrated by the constant average acceleration method that is second-order accurate, nondissipative and unconditionally stable; it is a member of the Newmark [20] family of methods.

For the free vibration problem, the frequency ω and the mode-shape vector $\bar{\delta}$ are solutions of the eigenvalue problem.

$$\mathbf{K}\bar{\delta} = \omega^2 \mathbf{M}\bar{\delta}. \tag{12}$$

Essential boundary conditions are imposed by modifying matrices \mathbf{M} and \mathbf{K} and the load vector \mathbf{F} ; see Refs. [9–11].

2.4. Optimization of natural frequencies

Frequencies of the FG plate depend upon material properties which are functions of the volume fractions of the two constituents given by Eq. (5). The volume fractions are controlled by parameters p and q . Hence $\omega = \omega(p, q)$. Thus the optimization problem reduces to finding

$p^* \in [0, p_{\max}]$ and $q^* \in [0, q_{\max}]$ so that

$$\omega(p^*, q^*) \geq \omega(p, q) \quad \text{for } 0 \leq p \leq p_{\max}, 0 \leq q \leq q_{\max}. \quad (13)$$

Here p_{\max} and q_{\max} are the maximum values of p and q . Eq. (13) is solved by the genetic algorithm [21].

3. Results and discussion

The first and the second natural frequencies have been optimized for an FG cantilever plate made of steel and aluminum, and $\ell = 200$ mm, $b = 50$ mm and $h = 20$ mm. The boundary conditions imposed are

$$u = v = w = 0 \quad \text{on } x = 0,$$

$$\bar{\mathbf{f}} = \mathbf{0} \quad \text{on surfaces } x = \ell, y = 0, y = b,$$

$$\mathbf{q}^{\pm} = 0 \quad \text{on } z = \pm h/2. \quad (14)$$

A computer code has been developed to analyze static deformations, and free and forced vibrations of a thick FG plate. It has been validated by comparing computed solutions with the analytical solution of the corresponding problems [9–11]. For simply supported homogeneous plates it also gives inplane modes of vibration [22].

Seventeen and five equally spaced nodes in the x - and y -directions, respectively, and $K = 5$ gave converged results. Thus for a free plate, the total number of degrees of freedom equals $3 \times 6 \times 85 = 1530$. The consistent mass matrix is used to analyze dynamic problems. Material properties assigned to steel and aluminum are as follows. Steel: $K_s = 166.67$ GPa, $\mu_s = 81.40$ GPa, $\rho_s = 7806$ kg/m³; aluminum: $K_a = 58.33$ GPa, $\mu_a = 26.92$ GPa, $\rho_a = 2707$ kg/m³. Results are presented in terms of the following nondimensional variables:

$$\bar{w} = \frac{50\mu_a h^3}{3\ell^4(1 - \nu_a)q_0} w, \quad \bar{\sigma}_{xx} = \frac{h^2 \sigma_{xx}}{\ell^2 q_0}, \quad \bar{\omega} = 100\omega h \sqrt{2\rho_a(1 + \nu_a)/\mu_a}, \quad (15)$$

where q_0 is the intensity of the uniformly distributed load applied on the top surface of the plate, and an overbar signifies a nondimensional quantity.

3.1. Optimized first two frequencies

For different values of exponents p and q in Eq. (6) we have listed in Table 1 the first ten natural frequencies of an FG cantilever plate. These results show that the first natural frequency of an FG plate is greater than that of a steel and an aluminum plate. For $p_{\max} = q_{\max} = 20$, we found that $p^* = 0$ and $q^* = 1.23$ make the first frequency largest which is 33.4% and 31% higher than the first frequency of an aluminum and a steel plate, respectively. The first ten frequencies for $p = 0$ and $q = 1.23$ are also listed in Table 1. It is clear that these values of p and q do not give largest values of the second through the tenth frequencies. The highest second nondimensional frequency of 6.80 is attained for $p = 0$ and $q = 4.70$ which is 9.08% and 7.01% greater than the second

Table 1

First ten nondimensional natural frequencies of a functionally graded cantilever plate for different compositional profiles

No	Aluminum	$p = 0$			$p = 2$			$p = 5$			Steel
		$q = 1.23$	$q = 2$	$q = 5$	$q = 0$	$q = 2$	$q = 5$	$q = 0$	$q = 2$	$q = 5$	
1	1.0362	1.3823	1.3582	1.2384	0.9687	1.1271	1.1030	0.9766	1.0875	1.0769	1.0552
2	2.4441	3.2513	3.2022	2.9369	2.4247	2.6652	2.6146	2.4579	2.5733	2.5494	2.4914
3	6.2369	6.7124	6.7465	6.8030	5.8664	6.3583	6.4323	5.9217	6.3047	6.3752	6.3580
4	6.5334	7.8046	7.7699	7.3885	6.2482	6.9432	6.8913	6.3182	6.7897	6.7852	6.6866
5	12.4698	13.5180	13.6080	13.6369	12.3342	12.8957	12.5990	12.5572	12.8043	12.8235	12.7270
6	15.7904	16.3552	16.5274	17.0662	15.3350	16.1797	16.3820	15.4924	16.1657	16.3442	16.0997
7	16.2388	18.8895	18.7661	17.7938	15.6707	16.7901	16.5667	15.8851	16.4367	16.4546	16.5566
8	19.7945	20.0365	20.2484	20.8825	18.9626	19.8838	20.2713	19.1844	19.8946	20.1836	20.2538
9	28.1302	28.3098	28.6636	29.5482	26.5860	28.1644	28.7056	26.8798	28.1161	28.5446	28.6780
10	28.8217	29.2323	29.5013	30.2469	28.6445	29.2523	29.5349	29.0349	29.3331	29.4703	29.4288

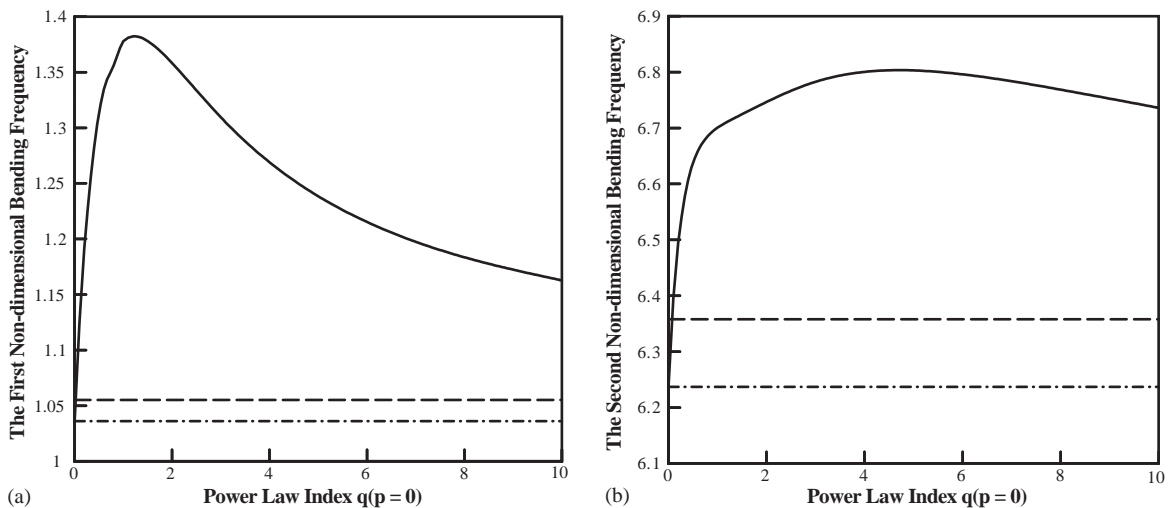


Fig. 2. Dependence upon the power-law index q of (a) the first and (b) the second nondimensional frequency of a functionally graded cantilever plate: — FGM; - - - -, aluminum; - - - -, steel.

frequency of aluminum and steel plates. Thus to maximize either the first or the second frequency, the composition of the plate needs to be varied in the axial direction rather than in the thickness direction. Furthermore, composition profiles for maximizing the two frequencies are different. Figs. 2(a) and (b) depict, respectively, the variation of the first and the second bending frequencies with the exponent q while $p = 0$. These confirm that the search algorithm gave correct values of q^* .

3.2. Forced transient response

The computed transient response of the FG cantilever plate loaded on the top surface by a uniformly distributed pressure of $100 \sin(1600t)$, where t is in seconds, is plotted in Fig. 3(a,b) for three sets of values of p and q . The time history of the tip deflection plotted in Fig. 3(a) reveals that there is no correlation between the first frequency and the amplitude of the tip deflection. For example, the ratio of the first frequency of the FG plate with $p = 0$ and $q = 1.23$ to that of aluminum and steel plates is about 1.3. However, the ratio of the maximum amplitude of the tip deflection of the FG plate to that of the aluminum plate is much less than that for the steel plate; for the latter it is close to 1.0. Frequencies of the forced response of the three plates are essentially the same. The time history of the axial stress at point B , with coordinates $(0, b/2, h/2)$, plotted in Fig. 3(b) reveals that the maximum axial stress induced in the FG plate is less than that in the two homogeneous plates.

For three sets of values of p and q , Fig. 4(a,b) shows time histories of the deflection of point A , with coordinates $(\ell, b/2, h/2)$, and of the axial stress at point B . Recall that $p = 0, q = 4.7$ maximizes the second natural frequency of the FG plate. In general, the maximum tip deflection and the maximum axial stress for the FG plate with $p = 0$ and $q = 4.7$ are lower than those for the other two plates with $(p, q) = (2, 2)$ and $(5, 5)$.

3.3. Static response

For $0 \leq p \leq p_{\max}$ and $0 \leq q \leq q_{\max}$, the steel plate has the highest value of Young's modulus. Thus the steel cantilever plate has the least tip deflection. However, the maximum axial stress at B is the same for all values of p and q . Numerical results confirmed this and are omitted.

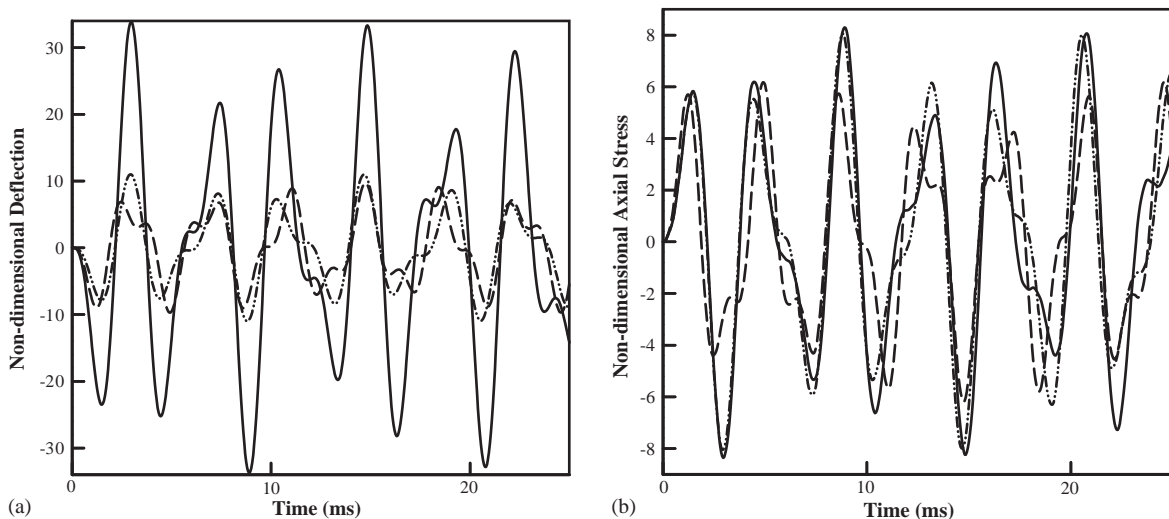


Fig. 3. For the bidirectional functionally graded cantilever plate loaded on the top surface by a uniformly distributed pressure of $10 \sin(1600t)$, time history of (a) the tip (point A in Fig. 1) deflection, and (b) the bending stress at point B (see Fig. 1 for location of point B): —, aluminum; - - - -, FGM ($p = 0, q = 1.23$); - · - · - ·, steel.

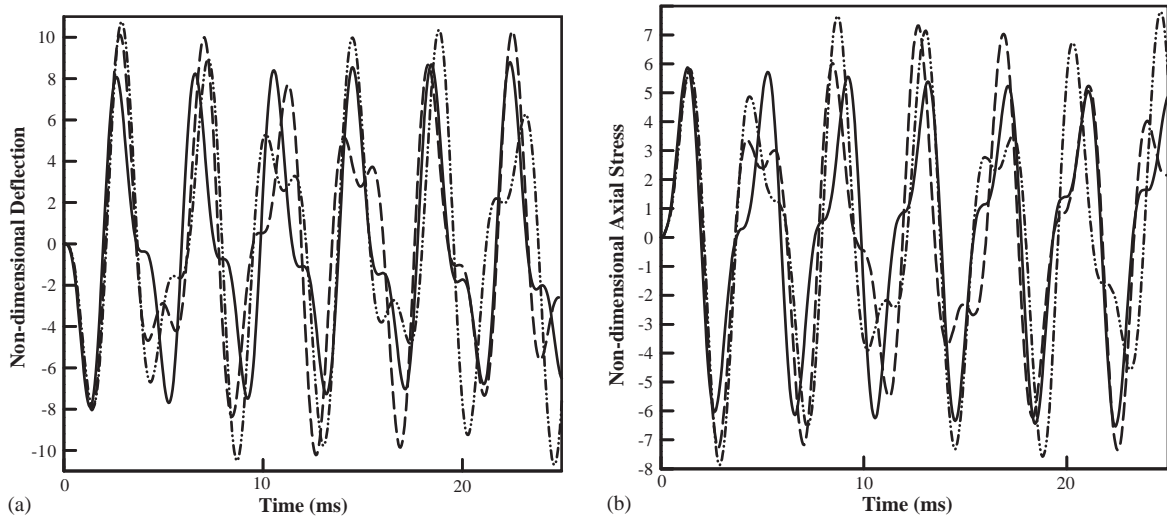


Fig. 4. For the bidirectional functionally graded cantilever plate loaded on the top surface by a uniformly distributed pressure of $10 \sin(1600t)$, time history of (a) the tip (point A in Fig. 1) deflection, and (b) the bending stress at point B (see Fig. 1 for location of point B): —, $p = 0$ $q = 4.7$; ---, $p = 2$ $q = 2$; - · - · - ·, $p = 5$ $q = 5$.

3.4. Remarks

The compositional profile obtained here for the maximum first or the second natural frequency is from the class of profiles given by Eq. (6) and the homogenization technique (5). A different homogenization method and another class of volume fraction variation may give results different from those obtained here. For example, Vel and Batra [23] have found that the Mori–Tanaka [18] and the self-consistent [24] methods of homogenizing material properties give different results for a simply supported FG plate. Also, we have kept the cross-section of the plate constant. The problem of finding the spatial variation of volume fractions of the two constituents and the cross-section of the plate to optimize a frequency is more challenging than the one analyzed here.

Vel and Batra [25] have given exact frequencies of a FG plate; these can be used to compare frequencies deduced from different plate theories. Batra and Jin [26] have analyzed the influence of the continuous variation of the fiber orientation angle through the plate thickness upon the natural frequencies of an anisotropic FG plate. It was found that dividing the plate into twenty layers of equal thickness simulated well the continuous through-the-thickness variation of the fiber orientation angle. A fully transient nonlinear coupled thermomechanical problem of the initiation of adiabatic shear bands in a FG microporous thermo-elasto-viscoplastic body has been scrutinized by Batra and Love [27].

4. Conclusions

We have used a higher-order shear and normal deformable plate theory and a meshless local Petrov–Galerkin method to find the compositional profile of a two-constituent cantilever plate so

that either the first or the second natural frequency is maximum. It is found that in each case, the composition varies only in the axial direction. The compositional profile for maximizing the first frequency is different from that for maximizing the second frequency. The forced transient response of each optimal functionally graded plate has been compared with that of the two homogeneous plates. The compositional profile that maximizes the first or the second natural frequency neither results in extreme values of the tip deflection nor in extreme values of the axial stress.

Acknowledgements

This work was partially supported by the ONR Grant N00014-98-1-0300 to Virginia Polytechnic Institute and State University with Dr. Y.D.S. Rajapakse as the program manager. L.F. Qian's work was also partially supported by the China Scholarship Council. Opinions expressed herein are those of the authors and not of the sponsoring agencies.

References

- [1] H.W. Lavendel, G.C. Goetzel, in: R.F. Hehemann, G.M. Ault (Eds.), *High Temperature Materials*, Wiley, New York, 1959, p. 140.
- [2] R. Berger, P. Kwon, C.K.H. Dharan, High speed centrifugal casting of metal matrix composites, in: *The Fifth International Symposium on Transport Phenomena and Dynamics of Rotating Machinery*, Maui, Hawaii, May 8–11, 1994.
- [3] Y. Fukui, Fundamental investigation of functionally gradient materials manufacturing system using centrifugal force, *JSME International Journal Series III* 34 (1991) 144–148.
- [4] K.-L. Choy, E. Felix, Functionally graded diamond-like carbon coatings on metallic substrates, *Materials Science and Engineering A* 278 (2000) 162–169.
- [5] K.A. Khor, Y.W. Gu, Effects of residual stress on the performance of plasma sprayed functionally graded ZrO/NiCoCr alloy coatings, *Materials Science and Engineering A* 277 (2000) 64–76.
- [6] A. Lambros, A. Narayanaswamy, M.H. Santare, G. Anlas, Manufacturing and testing of a functionally graded material, *Journal of Engineering Materials and Technology* 121 (1999) 488–493.
- [7] J.N. Reddy, Analysis of functionally graded plate, *International Journal for Numerical Methods in Engineering* 47 (2000) 663–684.
- [8] Z.Q. Cheng, R.C. Batra, Deflection relationships between the homogeneous Kirchhoff plate theory and different functionally graded plate theories, *Archive of Mechanics* 52 (2000) 143–158.
- [9] L.F. Qian, R.C. Batra, L.M. Chen, Elastostatic deformations of a thick plate by using a higher-order shear and normal deformable plate theory and two meshless local Petrov–Galerkin (MLPG) Methods, *Computer Modeling in Engineering and Sciences* 4 (2003) 161–176.
- [10] L.F. Qian, R.C. Batra, L.M. Chen, Free and forced vibrations of thick rectangular plates by using higher-order shear and normal deformable plate theory and meshless local Petrov–Galerkin (MLPG) Method, *Computer Modeling in Engineering and Sciences* 4 (2003) 519–534.
- [11] L.F. Qian, R.C. Batra, L.M. Chen, Static and dynamic deformations of thick functionally graded elastic plate by using higher-order shear and normal deformable plate theory and meshless local Petrov–Galerkin Method, *Composites: Part B* 35 (2004) 685–697.
- [12] R.C. Batra, S. Vidoli, Higher-order piezoelectric plate theory derived from a three-dimensional variational principle, *AIAA Journal* 40 (2002) 91–104.

- [13] R.C. Batra, S. Vidoli, F. Vestroni, Plane waves and modal analysis in higher-order shear and normal deformable plate theories, *Journal of Sound and Vibration* 257 (2002) 63–88.
- [14] S.N. Atluri, S.P. Shen, *The Meshless Local Petrov–Galerkin (MLPG) Method*, Tech. Science Press, 2002.
- [15] G.R. Liu, *Mesh Free Methods*, CRC Press, Boca Raton, FL, 2003.
- [16] L.F. Qian, R.C. Batra, Transient thermoelastic deformations of a thick functionally graded plate, *Journal of Thermal Stresses* 27 (2004) 705–740.
- [17] R.C. Batra, M. Porfiri, D. Spinello, Treatment of material discontinuity in two meshless local Petrov–Galerkin (MLPG) formulations of axisymmetric transient heat conduction, *International Journal for Numerical Methods in Engineering*, in press.
- [18] T. Mori, K. Tanaka, Average stress in matrix and average elastic energy of materials with misfitting inclusions, *Acta Metallurgica* 21 (1973) 571–574.
- [19] P. Lancaster, K. Salkauskas, Surfaces generated by moving least squares methods, *Mathematical Computation* 37 (1981) 141–158.
- [20] N.M. Newmark, A method of computation for structural dynamics, *Journal of Engineering Mechanics Division, ASCE* 85 (1959) 67–94.
- [21] D.E. Goldberg, *Genetic Algorithms in Search, Optimization and Machine Learning*, Addison-Wesley, Reading MA, 1989.
- [22] R.C. Batra, S. Aimmanne, Missing frequencies in previous exact solutions of free vibrations of simply supported plates, *Journal of Sound and Vibration* 265 (2003) 887–896.
- [23] S.S. Vel, R.C. Batra, Exact solution for thermoelastic deformations of functionally graded thick rectangular plates, *AIAA Journal* 40 (2002) 1421–1433.
- [24] R. Hill, A self-consistent mechanics of composite materials, *Journal of the Mechanics and Physics of Solids* 13 (1965) 213–222.
- [25] S.S. Vel, R.C. Batra, Three-dimensional exact solution for the vibration of functionally graded rectangular plates, *Journal of Sound and Vibration* 272 (2004) 703–730.
- [26] R.C. Batra, J. Jin, Natural frequencies of a functionally graded rectangular plate, *Journal of Sound and Vibration*, in press; doi:10.1016/j.jsv.2004.03.068.
- [27] R.C. Batra, B.M. Love, Adiabatic shear bands in functionally graded materials, *Journal of Thermal Stresses*, in press.